CORROSION SCIENCE AND TECHNOLOGY, Vol.22, No.2(2023), pp.99~107 pISSN 1598-6462 / eISSN 2288-6524
[Research Paper] DOI: https://doi.org/10.14773/cst.2023.22.2.99

Incorporation of Montmorillonite/Silica Composite for the Corrosion Protection of an Epoxy Coating on a 2024 Aluminum Alloy Substrate

Thai Thu Thuy, Trinh Anh Truc†, and Pham Gia Vu

Institute for Tropical Technology, Vietnam Academy of Science and Technology, 18 Hoang Quoc Viet, Hanoi 122000, Vietnam

(Received September 06, 2022; Revised November 16, 2022; Accepted November 16, 2022)

Layered silicate clay montmorillonite (MMT) has been used in nanocomposite coating to improve corrosion protection by reinforcing the barrier property. The better dispersion of MMT in the coating produces a higher barrier effect. Pretreatment with MMT could favor the delamination of clay platelets, facilitating MMT dispersion in the coating. In the present work, a montmorillonite/silica (MMT/Si) composite was prepared by the *in situ* sol-gel method. x-ray diffraction measurements and field-emission scanning electron microscopy observations showed silica crystal formation and increased basal spacing between the MMT platelets. Composite MMT/Si particles were introduced in an epoxy resin to reinforce the corrosion protection of the coating applied on the AA2024 surface. Electrochemical impedance spectroscopy (EIS) was performed to characterize the protective property of the coating. The results demonstrated the high barrier effect of the coating containing 5 wt% of MMT/Si. Adhesion evaluation after a salt spray test exhibited a high adherence to the epoxy coating containing MMT/Si.

Keywords: *Aluminum alloy, Montmorillonite, Silica, Corrosion protection, EIS*

1. Introduction

Nanoscale materials have been considered to improve their mechanical and barrier properties when dispersed into a polymer coating. This improvement is due to nanoparticles' large surface area, which provided good performance at low concentrations. Among the nanoparticles used in the polymer coating, sodium montmorillonite clay (MMT) attracted much attention thanks to its specific lamellar structure [1-3]. The completed separation of platelets (exfoliated state) in the polymer matrix leads to occlude of the micro tunnels. Therefore, it obstructs the pathway of water and corrosive species through the coating, resulting in an improving barrier effect [4-6]. Hence, the reinforcement effect depends on the dispersion level of clay platelets. To achieve this goal, MMT could be modified with an organic compound so that the platelets were intercalated for easy separation and, on the other hand, for better compatibility with organophilic polymer [7-10].

In the previous work, MMT was modified with organic corrosion inhibitors (modified-MMT) used in the primer to improve the corrosion protection of an epoxy coating on the steel surface. The enhancement was achieved by barrier reinforcement and corrosion inhibition at a low concentration of modified MMT (2-3%). However, since the total organic inhibitor content incorporated in the coating was very low (16% of inhibitor for 2% of inhibitor-MMT), long-term protection was suspected when being exposed to the aggressive medium [11-14].

Silica nanoparticles (nano-silica) were usually used in a clear coat to increase the scratch resistance; at low concentrations and uniform dispersion, the transparency or optical property was maintained [15-18]. The documents said that the addition of nano-silica in the epoxy coating exhibited better corrosion resistance than the micro particles due to the compact structure of chemical interaction of the hydroxyl groups of silica with epoxy resin. However, a surface modification is required to obtain a complete dispersion of nano-silica filler in the coating [19,20].

In the present work, nano-silica particles were deposited on the MMT platelets by a preparation in-situ in the sodium MMT to intercalate the MMT platelets (MMT/Si). The purpose is to increase the distance of MMT platelets to facilitate the dispersion in the polymer matrix and to improve the mechanical properties of the coating by taking advantage of both MMT and silica nanoparticles.

†Corresponding author: anhtruc.trinh@itt.vast.vn

2. Experimental

2.1 Materials

2024 aluminum alloy (AA2024) is supplied by Sonaca Company, Belgium. The coatings were applied on the AA2024 sheet with 4 × 6 × 0.1 cm dimension; before painting, the AA2024 samples were washed with absolute ethanol and dried.

The binder is water-based epoxy resin, composing YD828 as resin and Epicure 8537 as curing agents. The epoxy coating was deposited on the AA2024 surface by Filmfuge Paint Spinner Ref 110N (Sheen, United Kingdom) equipment.

2.1.1 Sodium silicate solution extra pure were from Merck

Sodium montmorillonite (Cloisite® 116, MMT) were supplied by BYK-Southern Clay product.

The synthesized MMT/Si was added to the epoxy at 1, 3, and 5 wt% concentration. MMT/Si particles were mechanically dispersed in a hardener for 1 hour before being incorporated into epoxy resin. The mixture was continuously stirred for 30 minutes and sonicated for 30 minutes to assure the completed dispersion of MMT/Si before scattering on pre-cleaned aluminum sheets (40 × 60 × 1 mm) with a rotating rate of 500 rpm for 20 seconds. The film thickness was approximately 30 ± 4 µm.

2.1.2 Preparation of the nano silica – montmorillonite clay (MMT/Si)

1 g of MMT was wholly dispersed in distilled water by agitation and then sonicated for 15-20 minutes to assure the exfoliation of MMT sheets, and then 7.1 g of $Na_2SiO_3.9H_2O$ were added to the suspension of MMT. The pH of the suspension was controlled at pH=2 by adjusting the H_2SO_4 2M solution. The hydrolysis was performed for 24 hours at room temperature, then at 80 ºC for 6 hours. The MMT/Si was collected by centrifuging (8000 rpm/ 5min) and repeatedly washed till pH = 7, then dried at 80 ºC in a vacuum oven overnight.

2.2. Analytical characterizations

The microstructure of synthesized MMT/Si was analyzed by X-ray diffraction (XRD, D5000 Siemens diffractometer (λCuKα = 1.5418 Å, 2θ steps = 0.015º/ step)) and Field-Emission Scanning Electron Microscope (FE-SEM, Hitachi S-4800)

The surface charge of the MMT and MMT/Si nanoparticles was determined using a Zeta Sizer SZ100-Z2 (Horiba Instrumentation). The MMT and MMT/Si powder were dispersed in distilled water by ultrasonic before being introduced into the Zeta cellule. A solution of KCl 10^{-3}M was used to set the ionic strength. Each sample was recorded at least 3 times to ensure a good statistic on the diagram distribution and the average surface charge values.

2.3. Electrochemical measurements

Electrochemical impedance spectroscopy (EIS) measurements were performed using three classical electrodes: the working electrode was the AA2024 panel, the reference electrode was an Ag/AgCl/KCl saturated, and the counter electrode was a platinum plate connecting with Biologic SP-300 equipment.

The EIS measurements were plotted at the frequency range from 100 kHz to 10 mHz at open circuit potential (OCP) with an amplitude of 10 mV. Each sample was realized at least three times to ensure the reproducibility of the measurement.

The salt spray test was performed according to ASTM B117 standard.

The coating adhesion was evaluated by the cross-hatch method following the ASTM D3359 standard. After 14 days of salt spray exposure, the samples were washed with distilled water and cleaned with cotton tissues before cutting; the samples were left at room temperature for 30 minutes to ensure a wholly dried state.

3. Results and discussions

3.1. Characterization of synthesized MMT/Si

The X-ray diffraction patterns between MMT and MMT/Si particles were compared in Fig. 1, in which the phase composition of both MMT and silica was determined.

The characteristic peak of silica detecting in the XRD pattern of MMT/Si represented the cristobalite form. 2θ value had been displaced to a minor angle from MMT to MMT/Si. The interlayer spacing of MMT d_{001} was calculated following Bragg's Law, which was 12 Å to 14 Å for MMT and MMT/Si, respectively. This XRD analysis demonstrated the formation of silica crystals on

the platelets of MMT, leading to an increase in the gallery distance of MMT.

The morphology of pristine MMT and synthesized MMT/Si is illustrated in Fig. 2.

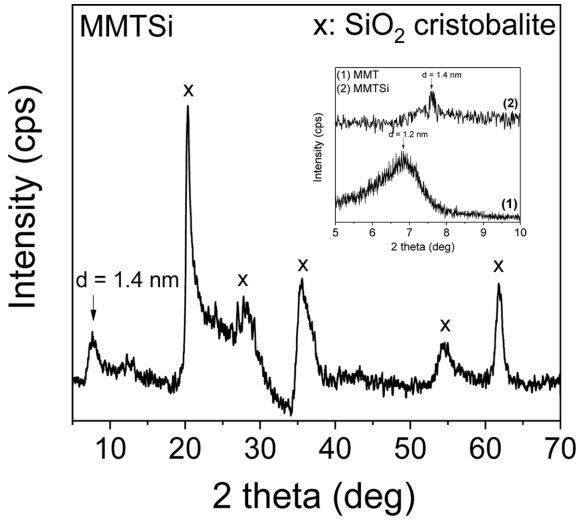

Fig. 1. X-ray diffraction patterns for MMT and MMT/Si particles

The layered structure of MMT was observed for both MMT and MMT/Si samples, but the MMT platelets were more expanded for the MMT/Si sample. SEM observation unifies with the XRD result, indicating an increase in the lamellate distance obtained for the MMT/Si sample.

The surface charge of MMT and MMT/Si was determined by Zeta potential measurement and presented in Fig. 3. Both MMT and MMT/Si presented a uniform surface charge distribution with a change of the average surface charge. It shifted to a more negative region from MMT to MMT/Si (-47 to -93 mV), indicating a modification of the surface state when precipitating silica on the MMT surface. The negative value of the surface charge could be attributed to the existence of hydroxyl group OH^- on the silica surface.

XRD, FESEM, and Zeta potential analysis identified that silica was successfully synthesized in the MMT solution; silica particles were distributed on the MMT platelets and expanded its layered distance.

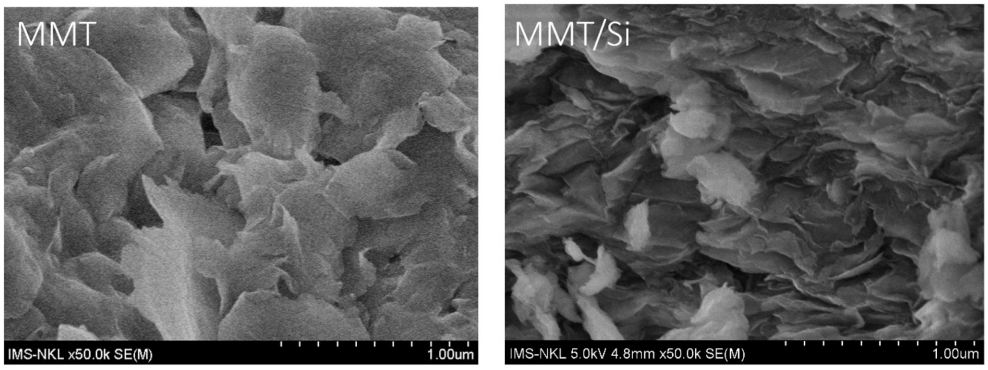

Fig. 2. FESEM images for MMT and MMT/Si particles

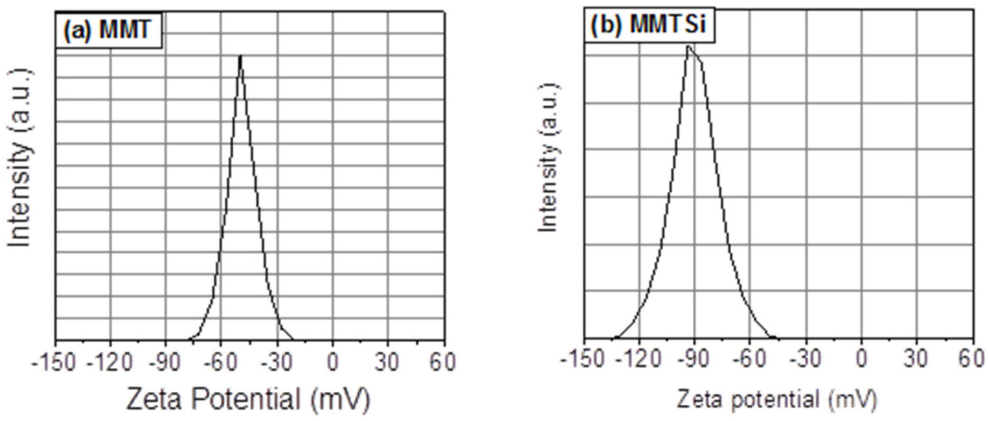

Fig. 3. Surface charge distribution of MMT and MMT/Si particles

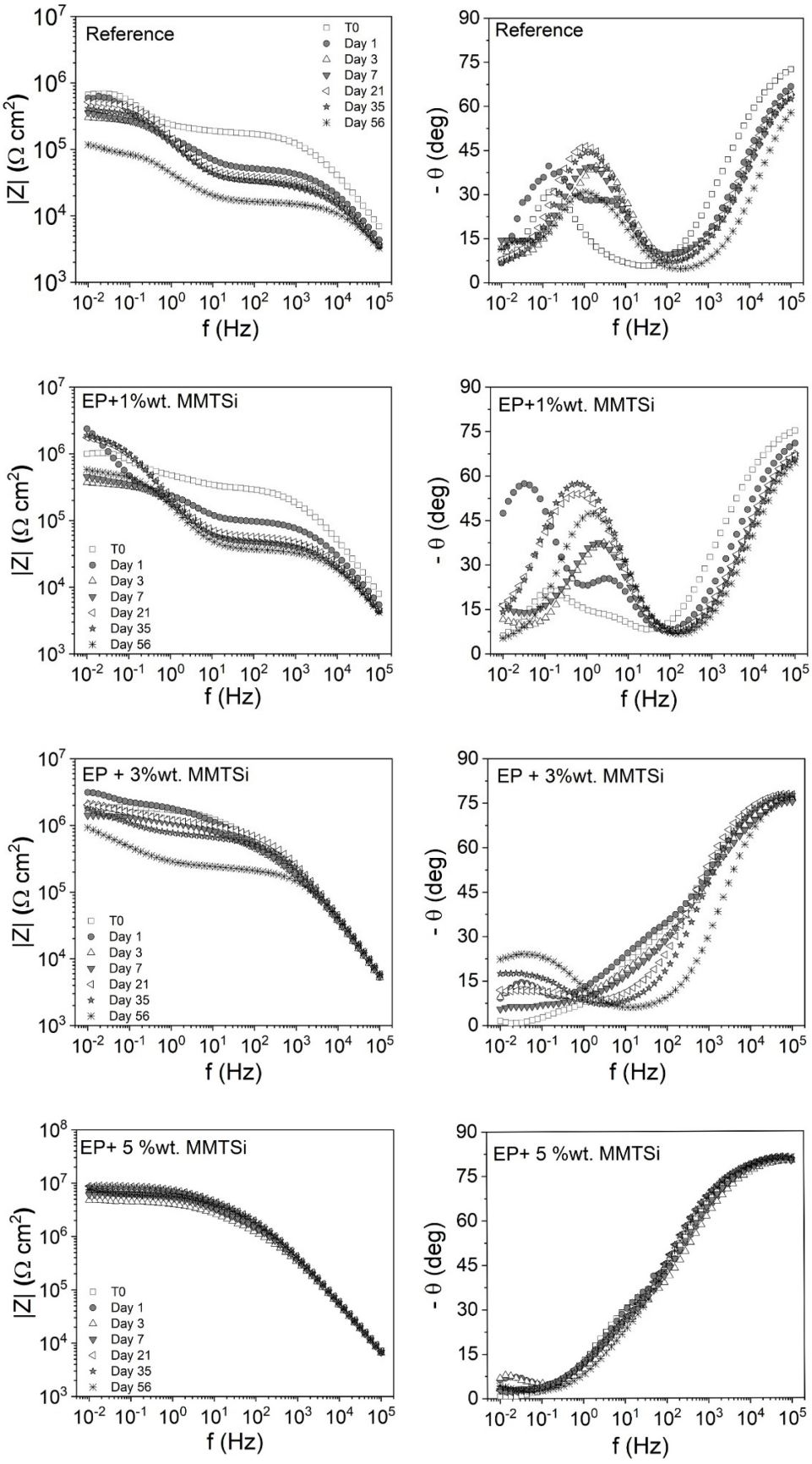

Fig. 4. Bode EIS diagrams for AA2024 surface covered by epoxy coating (reference) and the epoxy coating containing MMT/Si at different concentrations during immersion time in the electrolyte solution

3.2. Corrosion protection of epoxy coating containing MMT/Si

The protective property of the epoxy coating loading MMT/Si applied on the AA2024 surface had been characterized through EIS measurement during exposure to the NaCl 0.1 M solution. Fig. 4 showed Bode EIS diagrams of AA2024 sheets covered with epoxy and epoxy-containing MMT/Si at different concentrations. The coating epoxy loading MMT was not prepared due to the alkaline property of MMT, while MMT/Si was neutral in the aqueous milieu.

The EIS diagrams for the reference sample without pigment showed a modification associated with a decrease of high-frequency modulus on the first day, indicating the rapid degradation of the coating. For a short exposure time (1 day and 3 days), it exhibited 3-time constants well defined. The high-frequency part characterized the coating property; the middle part described the existence of the oxide layer, and the low part was characteristic of the Faradic process that occurred on the AA2024 surface. For a longer time, this low-frequency part disappeared due to the accumulation of corrosion products that sealed the micropores of the porous oxide.

Adding 1 wt% MMT/Si gave a similar form of reference sample, but the modulus values were slightly higher. For 3 wt% MMT/Si concentration, the EIS shapes remained relatively stable during 21 days with one time constant located at high frequency. A second-time constant appeared at a low frequency from 35 days (Fig. 4cc'), indicating an interfacial reaction occurred at the coating/metal interface. These EIS behaviors could be attributed to a barrier effect of the coating caused by the dispersion of the charge, which prolonged the diffusion path through the coating. At 5 wt% of MMT/Si (Fig. 4dd'), the EIS diagrams are unchanged during long exposure time in the electrolyte (56 days) with only one time constant. This stability of EIS diagrams indicated the high barrier property of the coating. It was mentioned in the literature that the exfoliated state of MMT in the coating leads to forming a tortuous path through the micropores of the coating, which slows down the diffusion process of the corrosion species to the metal surface [20].

It can be seen in Fig. 4a and 4b that three time-constants have early appeared from the initial exposure; for more prolonged exposure, the high-frequency behaviors can be distributed by the coating and the oxide layer under the

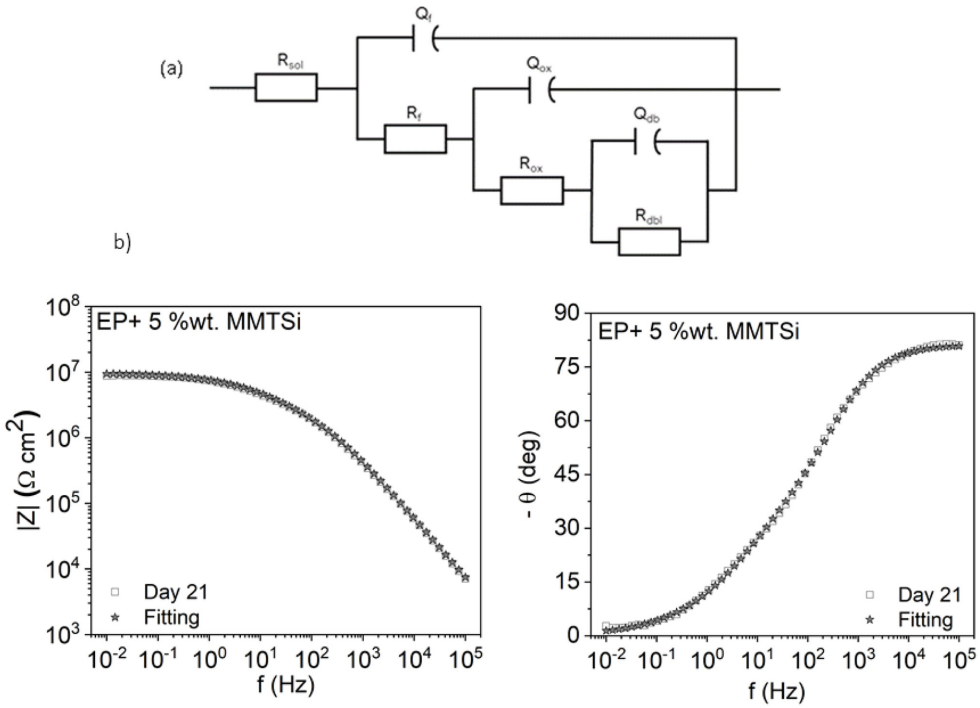

Fig. 5. Equivalent electric circuit (EEC) proposed for modeling the EIS data of AA2024 surface covered by epoxy coating and epoxy coating with MMT/Si (a) and Bode diagram for epoxy coating containing 5 wt% of MMT/Si after 21 days exposure in the NaCl 0.1 M

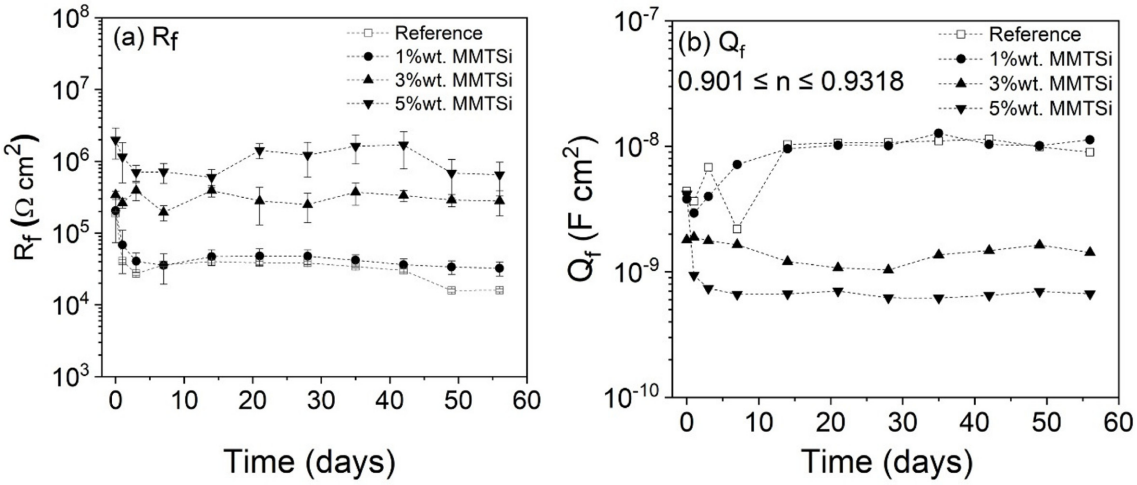

Fig. 6. Evolution of film resistance (R_f) and film CPE (Q_f) versus immersion time in the NaCl 0.1 M solution

coating. Therefore, an electrical equivalent circuit (EEC) with three-time constants was proposed for modeling the EIS data (Fig. 5a).

In this circuit, R_{sol} is electrolyte resistance; R_f is film resistance parallel connected with constant phase element (CPE, Q_f), which is the non-ideal capacitance of the coating. R_f connected in series with R_{ox} and Q_{ox} are characteristic of the existence oxide layer, and R_{dbl}, Q_{dbl} relate to charge transfer resistance and capacitance of the double layer. A comparison of experimental and fitting data for the epoxy coating loading 5 wt% of MMT/Si after 3 days of exposure was displayed in Fig. 5b, wherein the standard deviation of the fitting approximated ≤ 5%.

Fig. 6 showed the variation of coating resistance R_f and capacitance (Q_f) calculated from fitting data during immersion time in the electrolyte solution.

For a high concentration of MMT/Si (5 wt%), the film resistance values slightly decreased at the beginning and maintained stability till 56 days. For concentration of 3 wt%, it rested stable but at a lower value than the one at 5 wt%. The CPE value was low for the concentration of 5 wt% and higher for 3 wt%. At the weak content of MMT/Si (1 wt%), the variation of resistance and CPE was the same reference sample (without charge) with low film resistance and high film CPE values. Having published in the previous works that the incorporation of modified MMT in the epoxy coating improved the barrier property when exfoliated in the coating at 2–5 wt% [11-14]. It could be found in Fig. 1 and Fig. 2 that the formation of silica crystal on the MMT sheets led to expanding the lamellate structure of layered silicate and favored the dispersion of MMT/Si sheets in the coating. The MMT/silica ratio calculated in the MMT/Si approximated 1/1; therefore, it was in the optimal concentration range to obtain good dispersion in the epoxy coating.

Fracture surface observations were carried out for the epoxy coating, the epoxy coating containing 5 wt% of MMT/Si, and the analysis was compared with the coating loading 5 wt% pristine MMT. FESEM images of the fracture surface of the coating was displayed in Fig. 7. The surface of the epoxy coating without pigment is relatively smooth, while a rougher structure is observed for the epoxy coating loading MMT and MMT/Si. The dispersion of the MMT layers was clearly found, the accumulation was visible for the sample containing MMT, and it was well-separated for the sample with MMT/Si. Due to the aggregation, some voids and cavities appeared in the sample containing only MMT. The homogenous and exfoliated dispersion of MMT/Si in the epoxy coating signified a good miscible of MMT/Si. Moreover, interfacial adhesion between MMT/Si platelets with epoxy resin was remarked. This was due to silica particles on the silicate platelets, which could be more compatible with the polymer matrix. Then the increase of layered distance facilitated resin penetration to separate the lamellar layers.

The adhesion of the coating was evaluated after 14 days of salt fog exposure. It can be seen in Fig. 8 that the

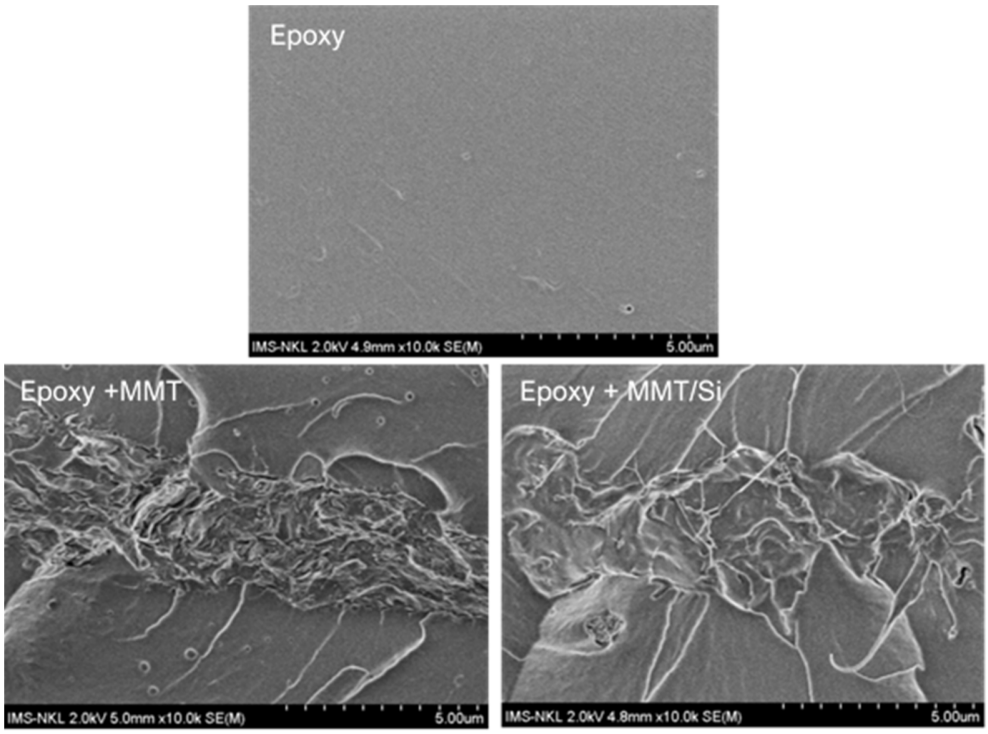

Fig. 7. FESEM cross-section images for epoxy coating, the epoxy coating containing 5 wt% of MMT and containing 5 wt% of MMT/Si

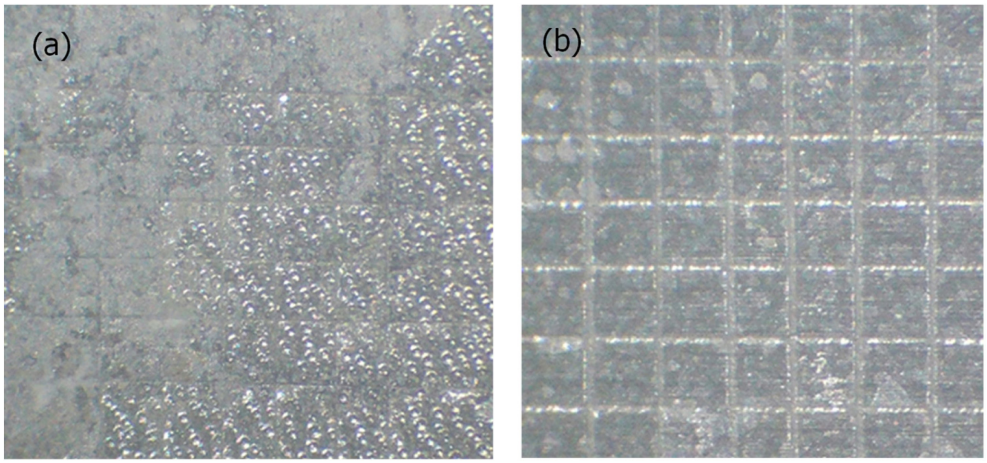

Fig. 8. Film adherence of epoxy coating (a) and the epoxy coating containing 5 wt% of MMT/Si (b) after 14 days of exposure to salt fog test

reference coating was seriously detached with a delaminated area of about 50%, indicating a poor adhesion of epoxy coating in salt fog conditions. On the contrary, for epoxy coating containing 5 wt% of MMT/Si, a few detachments were observed around squares incisions, demonstrating a good coating adherence. It was commented in the documents that the adsorption of water and oxygen on the coating/metal interface deteriorated the adhesion of the coating [21]. In this case, thanks to the barrier effect obtained by the presence of layered structure charge MMT/Si, the water penetration at the coating/interface was limited.

The EIS measurements linked to adhesion tests revealed that incorporating the MMT/Si composite in the epoxy coating applied on the AA2024 surface improved the barrier property of the coating. The high resistance and

low capacitance of the film were achieved while film adhesion was enhanced after 14 days of exposure to salt spray. This improvement could contribute to both roles of MMT and silica particles. In this case, the primary role of silica is to expand the layered distance of MMT, favoring the exfoliation of MMT in the epoxy resin.

4. Conclusions

Montmorillonite/silica composite was successfully synthesized in the aqueous medium; X-ray diffraction and FESEM analysis revealed the formation of crystal silica in the MMT platelets, which could expand the layered distance MMT. The introduction of MMT/Si into an epoxy coating at 3-5 wt% enhanced the corrosion protection mainly by improving the barrier effect and coating adhesion on the aluminum alloy 2024 surface. It can be seen that the high dispersion of MMT platelets in the epoxy coating was thanks to the deposition of silica on the MMT platelets.

Acknowledgements

The authors thank VAST for the funding support under project NVCC13.06/21-21

References

1. Richard A. Vaia, Gary Price, Patrick N. Ruth, Hieu T. Nguyen, Joseph Lichtenhan, Polymerr layered silicate nanocomposites as high performance ablative materials, *Applied Clay Science*, **15**, 67 (1999). Doi: https://doi.org/10.1016/S0169-1317(99)00013-7
2. Dongyan Wang, Charles A. Wilkie, In-situ reactive blending to prepare polystyrene–clay and polypropylene–clay nanocomposites, *Polymer Degradation and Stability*, **80**, 171 (2003). Doi: https://doi.org/10.1016/S0141-3910(02)00399-3
3. AijuanGua, Guozheng Liang, Thermal degradation behaviour and kinetic analysis of epoxy/montmorillonite nanocomposites, *Polymer Degradation and Stability*, **80**, 383– (2003). Doi: https://doi.org/10.1016/S0141-3910(03)00026-0
4. DavoodZaarei, Ali Asghar Sarabi, Farhad Sharif,Seid Mahmood Kassiriha, Structure, properties and corrosion resistivity of polymericnanocomposite coatings based on layered silicates, *Journal of Coatings Technology and Research*, **5**, 241 (2008). Doi: https://doi.org/10.1007/s11998-007-9065-5
5. Jui-Ming Yeh, Kung-Chin Chang, ReviewPolymer/layered silicate nanocomposite anticorrosive coatings, *Journal of Industrial and Engineering Chemistry*, **14**, 275 (2008). Doi: https://doi.org/10.1016/j.jiec.2008.01.011
6. Miloš D. Tomić, BrankoDunjić, Jelena B. Bajat,Violeta Likić, Jelena Rogan, JasnaDjonlagic, Anticorrosive epoxy/clay nanocomposite coatings: rheologicaland protective properties, *Journal Coatings Technology and Research*, **13**, 439 (2016). Doi: https://doi.org/10.1007/s11998-015-9762-4
7. Jui-Ming Yeha, Hsiu-Yin Huanga, Chi-Lun Chena, Wen-Fen Sua, Yuan-Hsiang Yu, Siloxane-modified epoxy resin–clay nanocomposite coatings with advanced anticorrosive properties prepared by a solution dispersion approach, *Surface and Coatings Technology*, **200**, 2753 (2006). Doi: https://doi.org/10.1016/j.surfcoat.2004.11.008
8. Rajkiran R. Tiwari, Kartic C. Khilar, Upendra Natarajan, Synthesis and characterization of novel organo-montmorillonites, *Applied Clay Science*, **38**, 203 (2008). Doi: https://doi.org/10.1016/j.clay.2007.05.008
9. LucileneBetega de Paiva, Ana Rita Morales, Francisco R. Valenzuela Díaz, Organoclays : Properties, preparation and applications, *Applied Clay Science*, **42**, 8 (2008). Doi: https://doi.org/10.1016/j.clay.2008.02.006
10. J. Y. Lee, H. K. Lee, Characterization of organobentonite used for polymer nanocomposites, *Materials Chemistry and Physics*, **85**, 410 (2004). Doi: https://doi.org/10.1016/j.matchemphys.2004.01.032
11. To Thi Xuan Hang, Trinh Anh Truc, Truong Hoai Nam, Vu Ke Oanh, Jean-Baptiste Jorcin, Nadine Pébère, Corrosion protection of carbon steel by an epoxy resin containing organically modified clay, *Surface and Coatings Technology*, **201**, 7408 (2007). Doi: https://doi.org/10.1016/j.surfcoat.2007.02.009
12. Trinh Anh Truc, To Thi Xuan Hang, Vu Ke Oanh, Eric Dantras, Colette Lacabanne, Djar Oquab, Nadine Pébère, Incorporation of an indole-3 butyric acid modified clay in epoxy resin for corrosion protection of carbon steel, *Surface and Coatings Technology*, **202**, 4945 (2008). Doi: https://doi.org/10.1016/j.surfcoat.2008.04.092
13. To Thi Xuan Hang, Trinh Anh Truc, Marie-Georges Olivier, Catherine Vandermiers, Nathalie Guérit, Nadine Pébère, Corrosion protection mechanisms of carbon steel by an epoxy resin containingindole-3 butyric acid modi-

fied clay, *Progress in Organic Coatings*, **69**, 410 (2010). Doi: https://doi.org/10.1016/j.porgcoat.2010.08.004

14. Trinh Anh Truc, Thai Thu Thuy, Vu Ke Oanh, To Thi Xuan Hang, Anh Son Nguyen, Nicolas Caussé, Nadine Pébère, 8-hydroxyquinoline-modified clay incorporated in an epoxy coating for the corrosion protection of carbon steel, *Surfaces and Interfaces*, **14**, 26 (2019). Doi: https://doi.org/10.1016/j.surfin.2018.10.007
15. Massoud Malaki, Yasser Hashemzadeh, Mehdi Karevan, Effect of nano-silica on the mechanical properties of acrylic polyurethane coatings, *Progress in Organic Coatings*, **101**, 477 (2016). Doi: https://doi.org/10.1016/j.porgcoat.2016.09.012
16. MassoudMalakia, Yasser Hashemzadeh, Alireza Fadaei Tehrani, Abrasion resistance of acrylic polyurethane coatings reinforced by nano silica, *Progress in Organic Coatings*, **125**, 507 (2018). Doi: https://doi.org/10.1016/j.porgcoat.2018.07.034
17. Tiina Nypelö, Monika Österberg, Xuejie Zu, Janne Laine, Preparation of ultrathin coating layers using surface modified silica nanoparticles, *Colloids and Surfaces A: Physicochemical and Engineering Aspects*, **392**, 313 (2011). Doi: https://doi.org/10.1016/j.colsurfa.2011.10.009
18. DeryaIşin, Nilhan Kayaman-Apohan, Atilla Güngör, Preparation and characterization of UV-curable epoxy/silica nanocomposite coatings, *Progress in Organic Coatings*, **65**, 477 (2009). Doi: https://doi.org/10.1016/j.porgcoat.2009.04.007
19. M. Rostami, Z. Ranjbar, M. Mohseni, Investigating the interfacial interaction of different aminosilane treated nano silicas with a polyurethane coating, *Applied Surface Science*, **257**, 899 (2010). Doi: https://doi.org/10.1016/j.apsusc.2010.07.087
20. Peter C. LeBaron, Zhen Wang, Thomas J. Pinnavaia, Polymer-layered silicate nanocomposites: an overview, *Applied Clay Science*, **15**, 11 (1999). Doi: https://doi.org/10.1016/S0169-1317(99)00017-4
21. V. V. Arslanov, W. Funke, The effect of water on the adhesion of organic coatings on aluminum, *Progress in Organic Coatings*, **15**, 355 (1988). Doi: https://doi.org/10.1016/0033-0655(88)85004-0